ELSEVIER

Clinical Imaging 35 (2011) 253–258

CLINICAL IMAGING

Multimodal imaging of recovery of functional networks associated with reversal of paradoxical herniation after cranioplasty ☆

Henning U. Voss[a,*], Linda A. Heier[b], Nicholas D. Schiff[c]

[a]Department of Radiology and Citigroup Biomedical Imaging Center, Weill Cornell Medical College, New York, NY 10021, USA
[b]Department of Radiology, Weill Cornell Medical College, New York, NY 10065, USA
[c]Department of Neurology and Neuroscience, Weill Cornell Medical College, New York, NY 10065, USA

Received 15 June 2010; accepted 16 July 2010

Abstract

Cranioplasty following decompressive craniectomy is reported to result in improved blood flow, cerebral metabolism, and concomitant neurological recovery. We used multimodal functional imaging technology to study a patient with marked neurological recovery after cranioplasty. Resting-state networks and auditory responses obtained with functional MRI and cerebral metabolism obtained with PET before and after cranioplasty revealed significant functional changes that were correlated with the subject's neurological recovery. Our results suggest a link between recovery of behavior, cerebral metabolism, and resting-state networks following cranioplasty.

Keywords: Cranioplasty; Resting-state functional MRI; Functional MRI; Positron emission tomography

1. Introduction

Management of patients after severe brain injury often includes the temporary removal of skull bone (craniectomy) in the acute stage to mitigate the effects of brain compression due to a variety of processes that may increase intracranial pressure. Replacement of the skull (cranioplasty) may lag the acute phase considerably, and case reports and case series have indicated that the cranioplasty procedure results in improved blood flow, cerebral metabolism, and concomitant neurological recovery [1–3]. More generally, recovery of integrative brain function after severe injuries resulting in a minimally conscious state (MCS) remains poorly understood, with behavioral recovery typically occurring over many months [4] or even years [5]. As a result of the slow time course of recovery and the potential for cognitive recovery to proceed in the absence of overt motor behavior [6], it is increasingly recognized that quantitative neurofunctional measures are needed to more precisely track the evolution of recovery [7,8]. Here, we obtained functional MRI (fMRI) auditory response, resting-state networks (RSNs), and fluorodeoxyglucose positron emission tomography (FDG-PET) before and after right hemispheric cranioplasty in a subject with severe brain injury who emerged from MCS following the procedure.

In resting-state fMRI, subjects undergo a conventional fMRI imaging protocol without performing specific cognitive or motor tasks. The resulting blood-oxygen-level-dependent (BOLD) signal contains various RSN patterns obtained by algorithms that compute and segment correlations in the signal [9–12] and that putatively reveal information about connectivity of the cerebral neurovascular network. Although neither the physiological origins of

☆ Design and conduct of the study; collection, management, analysis, and interpretation of the data; and preparation, review, or approval of the manuscript were supported by the National Institutes of Health National Institute of Child Health and Human Development, the James S. McDonnell Foundation (N.D.S.), the Institute for Biomedical Imaging Sciences, and a Fleming Award from Weill Cornell Medical College (H.U.V).

* Corresponding author. Department of Radiology and Citigroup Biomedical Imaging Center, Weill Cornell Medical College, 516 E 72nd St., New York, NY 10021, USA. Tel.: +1 212 746 5216 (office, msg. box), +1 212 746 5702 (lab); fax: +1 212 746 6681.

E-mail addresses: hev2006@med.cornell.edu (H.U. Voss), laheier@med.cornell.edu (L.A. Heier), nds2001@med.cornell.edu (N.D. Schiff).

0899-7071/$ – see front matter © 2011 Elsevier Inc. All rights reserved.
doi:10.1016/j.clinimag.2010.07.008

resting-state signals nor their potential clinical utility has been completely characterized yet, a broad array of clinical applications of resting-state fMRI has been investigated during the past 5 years [13]. The most prominent RSN, the "default mode," was originally discovered in resting metabolism (PET) data [12] and later confirmed in conventional fMRI studies [14], and it is thought to reflect the existence of an organized, baseline default mode of brain function. It is also thought to be involved in consciousness on a more basic level since it partially disintegrates during deep sleep [15]. In addition to the default mode network, several other RSNs have been identified more recently [16,17], and a direct correspondence has been demonstrated between their BOLD signals and fluctuations in EEG oscillations [16,18–20]. Furthermore, theoretical modeling attempts of the dynamics of RSNs, for example, by means of numerical coupled oscillator networks [21], will lead to a deeper understanding of the relationship of clinical RSN observations and pathologies of intrinsic brain dynamics, such as disturbances in conduction delays.

1.1. Case report

Six months prior to the first imaging study reported herein, the subject, a 19-year-old woman, suffered a severe traumatic brain injury following a fall from the front of a moving vehicle. Initial examination in the field revealed signs of central herniation with bilateral pupillary dysfunction with a Glasgow Coma Scale score of 3. Emergency management included acute evacuation of a left epidural hematoma and bilateral craniotomies. Intracranial pressure monitoring showed an average intracranial pressure of 30 mmHg. Over the next 5 months following acute injury, the patient demonstrated inconsistent evidence of response to environmental stimuli as documented in medical records that did not improve after placement of a ventriculoperitoneal shunt in the second month after injury. One month prior to the first imaging study, the patient underwent a left-sided cranioplasty with subsequent recovery of reliable command following to simple motor commands. On admission to our study, the patient's neurological exam was notable for 4-mm pupils bilaterally reactive to 2 mm, a left upward gaze preference with occasional spontaneous nystagmus, and increased range of movement to the left with passive oculocephalic stimulation. Grip strength of 2/5 was noted bilaterally with no withdrawal of the right upper extremity to noxious stimuli and spontaneous withdrawal of the left upper extremity; lower extremities revealed bilateral spastic contractures with hyperreflexia. Formal quantitative behavioral assessment at the time of the first study reported here demonstrated an exam consistent with MCS, including reliable auditory command following and intermittent gestural communication. The Coma Recovery Scale Revised [22] best total score was 14 (patient demonstrated consistent following of auditory commands, visual tracking despite a lack of blink to direct threat, object manipulation with the right hand, absence of vocalization or oral movement, inconsistent and inaccurate "yes"/ "no" responses with right thumb, and eyes in open state without stimulation). The second imaging study was done 10 months after injury and 2 months following a right-sided cranioplasty. At this time, the patient demonstrated further improvements on quantitative behavioral examination, including recovery of functional object use (demonstrated using her right hand and upper extremity of the function use of common objects), vocalization to command, consistent communication (accurate "yes"/ "no" responses through gesture), and improved attentional function with consistent responses to examiner queries (Coma Recovery Scale Revised total score of 20). At the time of this second evaluation, formal testing indicated emergence from MCS based on sequential examination demonstrating consistent and accurate communication on simple situational accuracy questions.

2. Materials and methods

An institutional-review-board-approved consent declaration was obtained from the patient's legally authorized surrogate under active approved protocols. The imaging protocols for both study time points were identical. Resting-state fMRI and auditory fMRI were performed, together with anatomical MRI, on a 3.0-Tesla General Electric Medical Systems (Waukesha, WI) clinical MRI system with an eight-channel head coil using echo-planar-imaging-based fMRI pulse sequences (repetition time=2 s, echo time=30 ms, flip angle=70°, matrix size=64×64×28, axial field of view=24 cm, 5-mm slice thickness; resting-state fMRI was acquired with 180 samples, whereas auditory fMRI was acquired with 128 samples). Before resting-state fMRI, the subject was instructed to think of nothing in particular; during auditory fMRI, the subject was instructed over headphones to imagine herself swimming and to stop imagining herself swimming, for eight times each. The data were analyzed with BrainVoyager QX (Brain Innovation, The Netherlands; motion correction, smoothing, detrending, resampling) and by using independent component analysis (resting-state fMRI) and general linear modeling (auditory fMRI) including

Fig. 1. Top four rows: RSNs before (left column) and after (right column) cranioplasty. The auditory-phonological network could not be identified by independent component analysis before cranioplasty and emerges only post-surgery. Colors denote *z*-values for the independent components as shown on the scale in the third row on the left. Bottom row: Auditory responses to stimulation with short spoken sentences before (left) and after (right) cranioplasty. Before cranioplasty, auditory response was absent on the ipsilateral side and restored after cranioplasty. Colors denote *z*-values of the general linear model used to fit the response. The threshold is defined as a false discovery rate of the multiple test problem of P=.05. Dashed lines on the axial cuts denote the position of the corresponding sagittal images. Axial cuts are shown in radiological convention in which the right side of the brain is shown on the left side of the image.

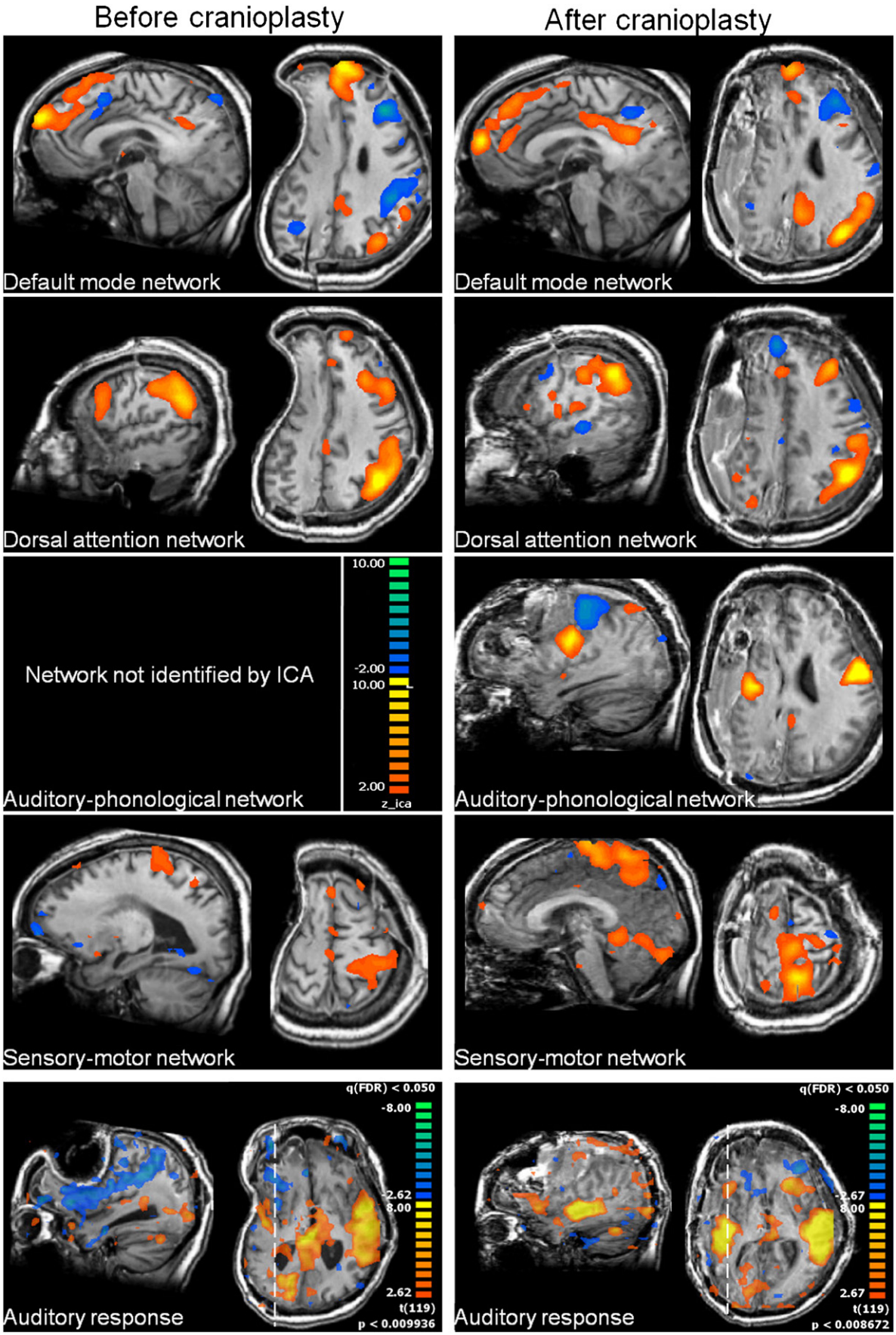
Before cranioplasty
After cranioplasty
Default mode network
Default mode network
Dorsal attention network
Dorsal attention network
Network not identified by ICA
10.00
-2.00
10.00
2.00
z_ica
Auditory-phonological network
Auditory-phonological network
Sensory-motor network
Sensory-motor network
q(FDR) < 0.050
-8.00
-2.62
8.00
2.62
t(119)
p < 0.009936
Auditory response
q(FDR) < 0.050
-8.00
-2.67
8.00
2.67
t(119)
p < 0.008672
Auditory response

motion parameters as nuisance variables. In this model, the auditory instructions (and not the imagery periods in between) were used as stimuli. Fluorine-18 FDG-PET was performed on a General Electric Medical Systems combined PET-CT LS Discovery unit. Images were acquired in dynamic high-sensitivity emission mode (matrix size=128×128×35, axial field of view=25 cm, 4.25-mm slice thickness). Standard uptake values (SUVs) were computed from the PET data including CT-based skull attenuation corrections and then co-registered to high-resolution MRI images using PMOD (PMOD Technologies Ltd., Switzerland) and visualized using Mricron (Chris Rorden).

3. Results

3.1. Anatomical changes

Before cranioplasty, anatomical MRI showed an overall loss of brain symmetry due to distortions with marked evidence of sunken skin flap depression on the side of the craniectomy (Fig. 1, left panels). T1-weighted images showed hyperintense cortical contusion with laminar necrosis. T2-weighted FLAIR images showed anterior temporal, inferior frontal, and bilateral occipital injury. After cranioplasty, symmetry seemed to be only slightly restored. Structural imaging showed serosanguinous collection underlining cranioplasty and new small subdural collections surrounding both hemispheres (Fig. 1, right panels). A detailed comparison of the two brain images after co-registration revealed that ventricular spaces were markedly reduced after cranioplasty (not shown).

3.2. RSN changes

Of the six RSNs described in Ref. [16], in this subject, three networks were found before and after cranioplasty, namely the default mode network, the dorsal attention network, and the sensory-motor network. The visual and self-referential networks could not be found in either case. The auditory-phonological network only showed up post-cranioplasty. Parametric maps of RSN connectivity are provided in Fig. 1. [For comparison, a study with nine normal control subjects using the same methodology resulted in a 93% reliability of network identification (H.U.V., unpublished data)]. Overall, the networks that existed at both time points increased in volume or remained unchanged: default mode network, +40% (from 52 to 73 ccm); dorsal attention network, −2% (from 56 to 55 ccm); and sensory-motor network, +46% (from 67 to 98 ccm).

3.3. Auditory response changes

Before cranioplasty, auditory responses to short spoken sentences were found mainly in left primary auditory areas and were mostly absent on the side of the craniectomy. After cranioplasty, strong auditory responses were found bilaterally (Fig. 1, bottom two rows).

3.4. Resting metabolism changes

A marked increase in SUVs of FDG was observed after cranioplasty. Whole-brain-averaged SUVs (excluding the cavity at the second time point) increased from 2.5±2.0 to 3.0±2.4 g/ml (±standard deviation). Regional changes

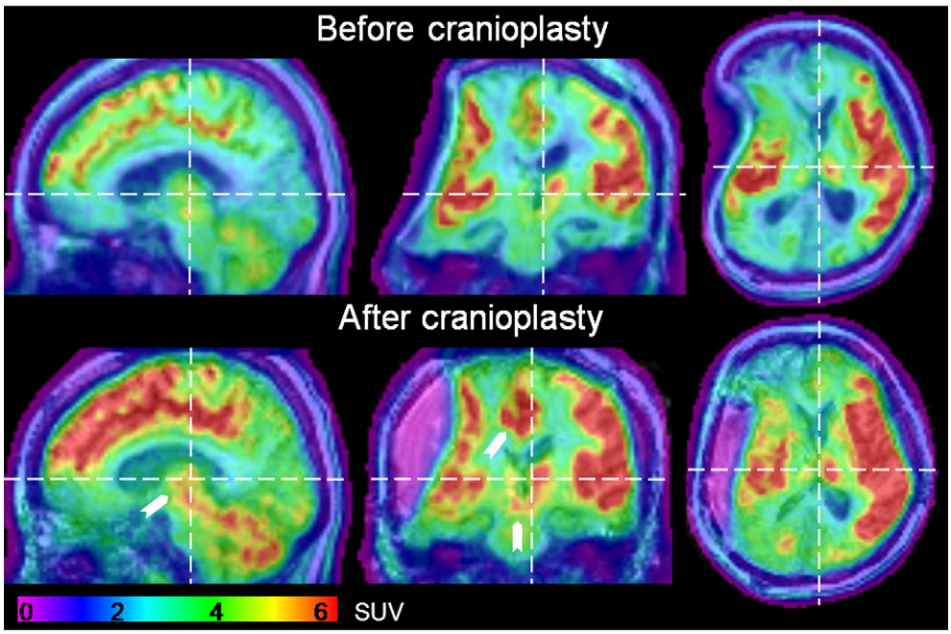

Fig. 2. FDG-PET images before and after cranioplasty overlaid onto anatomical MRI images. Color-coded SUVs in units of grams per milliliter as shown in the color bar at the bottom of the panel and arrows point toward changes in the mesodiencephalic and mesial cortical regions. Dashed lines mark the position of the corresponding other cuts. Axial and coronal cuts are shown in radiological convention.

were observed in left mesial frontal regions and within the mesodiencephalon (upper brainstem and thalamus) (Fig. 2, arrows).

4. Discussion

We have found signatures of increased functional activity using three functional imagining modalities in a subject following cranioplasty to repair a sinking flap produced after decompressive craniectomy. FDG-PET measurements indicated both global increases in cerebral metabolism and marked local improvements in the mesodiencephalic region; resting-state fMRI and auditory fMRI revealed more specific information about neuronal network functional connectivity. We have previously identified loss of RSNs in the setting of specific neurovascular injuries [13] with lesioned neuronal substrates, but the reappearance of the auditory RSN after cranioplasty along with a significantly enhanced auditory response on the ipsilateral side is novel and points toward further clinical significance of RSN imaging in addition to previous findings. Some RSNs are robust to anesthesia [23,24] and light sleep [25], suggesting that intrinsic neurovascular coupling contributes to them. Prior studies have identified reversible changes in neurovascular coupling using electroencephalography measures and FDG-PET in the MCS [26]. Taken together, these observations may relate to aspects of recovery of cerebral autoregulation mechanisms and raise the possibility that RSNs per se reflect a key aspect of the spatiotemporal regulation of intracranial blood volume, observed as the constancy of cerebral blood pressure across wide ranges of systemic blood pressures.

Our finding of reduced RSN connectivity on the side of the craniectomy can be directly related to a prior demonstration of reduced EEG network coherence in the lesioned hemisphere in a vegetative patient with severe asymmetric subcortical brain damage associated with the loss of thalamic input [27]. Measurement of RSNs is based on the coherence of BOLD signals, and both findings may reflect damage to thalamocortical loop connections, likely a strong source of EEG coherence [28] and of RSN connectivity [29,30]. Improvement in the auditory RSN seen here may thus associate with our findings of reversal of depressed resting metabolism in the thalamus following cranioplasty.

Subject motion can conceal functional activations and RSN components and should always be considered in interpreting data from subjects who are not fully cooperative and thus on average move more than healthy control subjects. In this study, head motion was more pronounced at the second time point for the functional scan and at the first time point for the resting-state scan. Therefore, it cannot account for the common trend observed in both scans alone.

The marked increase in regional cerebral metabolism (FDG-PET) in the left mesial frontal regions and within the mesodiencephalon of the left hemisphere before and after the cranioplasty is of particular note. This finding suggests a partial resolution of a component of "paradoxical herniation" originating from the earlier craniectomy. Prior studies have demonstrated a mesodiencephalic herniation syndrome resulting from the effects of atmospheric pressure and gravity in the setting of craniectomy [31–33].

Bilateral improvements of regional cerebral blood flow after cranioplasty have been shown before in perfusion [3], dynamic [34], and xenon-enhanced [35] CT imaging. Our study demonstrates the potential utility of resting-state MRI and fMRI, both of which can be easily added to conventional clinical MRI protocols without the need for an additional imaging session. In our patient, significant increases in the volume of some RSN components and both global and regional cerebral metabolism measured using FDG-PET correlated with the subject's neurological recovery. Notably, the auditory RSN, absent before cranioplasty, reappeared afterwards, a novel observation that suggests a link between intrinsic brain mechanisms of cerebral vascular integration and the RSN response. The findings support the role of cranioplasty in restoring aspects of integrative cerebral function after severe brain injuries and provide further insight into the physiological basis of RSNs.

Our results suggest the potential utility of these functional measures to track recovery following decompressive craniectomy procedures; the procedure has become an increasingly frequent part of the neurocritical care of patients with severe brain injury and has wide application in the clinical management of increased intracranial pressure arising in the setting of different types of brain insult [31]. Such physiological assessments of recovery during post-operative management after craniectomies are likely to be particularly important for patients with severe brain injuries or the elderly who may recover slowly from their injuries [36].

Acknowledgments

We thank Lauren Rissman for data analysis support.

References

[1] Isago T, Nozaki M, Kikuchi Y, Honda T, Nakazawa H. Sinking skin flap syndrome: a case of improved cerebral blood flow after cranioplasty. Ann Plast Surg 2004;53(3):288–92.
[2] Winkler PA, Stummer W, Linke R, Krishnan KG, Tatsch K. The influence of cranioplasty on postural blood flow regulation, cerebrovascular reserve capacity, and cerebral glucose metabolism. Neurosurg Focus 2000;8(1):e9.
[3] Sakamoto S, Eguchi K, Kiura Y, Arita K, Kurisu K. CT perfusion imaging in the syndrome of the sinking skin flap before and after cranioplasty. Clin Neurol Neurosurg 2006;108(6):583–5.
[4] Lammi MH, Smith VH, Tate RL, Taylor CM. The minimally conscious state and recovery potential: a follow-up study 2 to 5 years after traumatic brain injury. Arch Phys Med Rehabil 2005;86(4):746–54.
[5] Voss HU, Ulug AM, Dyke JP, Watts R, Kobylarz EJ, McCandliss BD, Heier LA, Beattie BJ, Hamacher KA, Vallabhajosula S, Goldsmith SJ, Ballon D, Giacino JT, Schiff ND. Possible axonal regrowth in late recovery from the minimally conscious state. J Clin Invest 2006;116(7):2005–11.

[6] Owen AM, Coleman MR, Boly M, Davis MH, Laureys S, Pickard JD. Detecting awareness in the vegetative state. Science Sept.2006;313 (5792):1402.
[7] Laureys S, Giacino JT, Schiff ND, Schabus M, Owen AM. How should functional imaging of patients with disorders of consciousness contribute to their clinical rehabilitation needs? Curr Opin Neurol 2006;19(6):520–7.
[8] Schiff ND. Measurements and models of cerebral function in the severely injured brain. J Neurotrauma 2006;23(10):1436–49.
[9] Formisano E, Esposito F, Kriegeskorte N, Tedeschi G, Di Salle F, Goebel R. Spatial independent component analysis of functional magnetic resonance imaging time-series: characterization of the cortical components. Neurocomputing 2002;49:241–54.
[10] Biswal B, Yetkin FZ, Haughton VM, Hyde JS. Functional connectivity in the motor cortex of resting human brain using echo-planar MRI. Magn Reson Med 1995;34(4):537–41.
[11] Fox MD, Snyder AZ, Vincent JL, Corbetta M, Van Essen DC, Raichle ME. The human brain is intrinsically organized into dynamic, anticorrelated functional networks. Proc Natl Acad Sci U S A 2005; 102(27):9673–8.
[12] Raichle ME, MacLeod AM, Snyder AZ, Powers WJ, Gusnard DA, Shulman GL. A default mode of brain function. Proc Natl Acad Sci U S A 2001;98(2):676–82.
[13] Voss HU, Schiff ND. MRI of neuronal network structure, function, and plasticity. Prog Brain Res 2009;175:483–96.
[14] Singh KD, Fawcett IP. Transient and linearly graded deactivation of the human default-mode network by a visual detection task. Neuroimage 2008;41(1):100–12.
[15] Horovitz SG, Braun AR, Carr WS, Picchioni D, Balkin TJ, Fukunaga M, Duyn JH. Decoupling of the brain's default mode network during deep sleep. Proc Natl Acad Sci U S A 2009;106(27):11376–81.
[16] Mantini D, Perrucci MG, Del Gratta C, Romani GL, Corbetta M. Electrophysiological signatures of resting state networks in the human brain. Proc Natl Acad Sci U S A 2007;104(32):13170–5.
[17] De Luca M, Beckmann CF, De Stefano N, Matthews PM, Smith SM. fMRI resting state networks define distinct modes of long-distance interactions in the human brain. Neuroimage 2006;29(4):1359–67.
[18] Goldman RI, Stern JM, Engel J, Cohen MS. Simultaneous EEG and fMRI of the alpha rhythm. Neuroreport 2002;13(18):2487–92.
[19] Laufs H, Krakow K, Sterzer P, Eger E, Beyerle A, Salek-Haddadi A, Kleinschmidt A. Electroencephalographic signatures of attentional and cognitive default modes in spontaneous brain activity fluctuations at rest. Proc Natl Acad Sci U S A 2003;100(19):11053–8.
[20] Lu H, Zuo Y, Gu H, Waltz JA, Zhan W, Scholl CA, Rea W, Yang Y, Stein EA. Synchronized delta oscillations correlate with the resting-state functional MRI signal. Proc Natl Acad Sci U S A 2007;104(46): 18265–9.
[21] Deco G, Jirsa V, McIntosh AR, Sporns O, Kotter R. Key role of coupling, delay, and noise in resting brain fluctuations. Proc Natl Acad Sci U S A 2009;106(25):10302–7.
[22] Giacino JT, Kalmar K, Whyte J. The JFK Coma Recovery Scale-Revised: measurement characteristics and diagnostic utility. Arch Phys Med Rehabil 2004;85(12):2020–9.
[23] Vincent JL, Patel GH, Fox MD, Snyder AZ, Baker JT, Van Essen DC, Zempel JM, Snyder LH, Corbetta M, Raichle ME. Intrinsic functional architecture in the anaesthetized monkey brain. Nature 2007;447 (7140):83–6.
[24] Boly M, Phillips C, Tshibanda L, Vanhaudenhuyse A, Schabus M, ng-Vu TT, Moonen G, Hustinx R, Maquet P, Laureys S. Intrinsic brain activity in altered states of consciousness: how conscious is the default mode of brain function? Ann N Y Acad Sci 2008;1129: 119–29.
[25] Horovitz SG, Fukunaga M, de Zwart JA, van GP, Fulton SC, Balkin TJ, Duyn JH. Low frequency BOLD fluctuations during resting wakefulness and light sleep: a simultaneous EEG-fMRI study. Hum Brain Mapp 2008;29(6):671–82.
[26] Coleman MR, Menon DK, Fryer TD, Pickard JD. Neurometabolic coupling in the vegetative and minimally conscious states: preliminary findings. J Neurol Neurosurg Psychiatry 2005;76(3): 432–4.
[27] Davey MP, Victor JD, Schiff ND. Power spectra and coherence in the EEG of a vegetative patient with severe asymmetric brain damage. Clin Neurophysiol 2000;111(11):1949–54.
[28] Contreras D, Destexhe A, Sejnowski TJ, Steriade M. Control of spatiotemporal coherence of a thalamic oscillation by corticothalamic feedback. Science 1996;274(5288):771–4.
[29] Martuzzi R, Ramani R, Qiu M, Rajeevan N, Constable RT. Functional connectivity and alterations in baseline brain state in humans. Neuroimage 2009.
[30] Zhang D, Snyder AZ, Shimony JS, Fox MD, Raichle ME. Noninvasive functional and structural connectivity mapping of the human thalamocortical system. Cereb Cortex 2009.
[31] Akins PT, Guppy KH. Sinking skin flaps, paradoxical herniation, and external brain tamponade: a review of decompressive craniectomy management. Neurocrit Care 2008;9(2):269–76.
[32] Oyelese AA, Steinberg GK, Huhn SL, Wijman CA. Paradoxical cerebral herniation secondary to lumbar puncture after decompressive craniectomy for a large space-occupying hemispheric stroke: case report. Neurosurgery 2005;57(3):E594.
[33] Fields JD, Lansberg MG, Skirboll SL, Kurien PA, Wijman CA. "Paradoxical" transtentorial herniation due to CSF drainage in the presence of a hemicraniectomy. Neurology 2006;67(8):1513–4.
[34] Suzuki N, Suzuki S, Iwabuchi T. Neurological improvement after cranioplasty. Analysis by dynamic CT scan. Acta Neurochir (Wien) 1993;122(1–2):49–53.
[35] Maekawa M, Awaya S, Teramoto A. (Cerebral blood flow (CBF) before and after cranioplasty performed during the chronic stage after decompressive craniectomy evaluated by xenon-enhanced computerized tomography (Xe-CT) CBF scanning)No Shinkei Geka 1999;27 (8):717–22.
[36] Crossley M, Shiel A, Wilson B, Coleman MR, Gelling L, Fryer T, Boniface S, Pickard J. Monitoring emergence from coma following severe brain injury in an octogenarian using behavioural indicators, electrophysiological measures and metabolic studies: a demonstration of the potential for good recovery in older adults. Brain Inj 2005;19(9): 729–37.